




## Article

# Glikinite, $Zn_3O(SO_4)_2$ , a new anhydrous zinc oxysulfate mineral structurally based on $OZn_4$ tetrahedra.

Evgeny V. Nazarchuk<sup>1</sup>, Oleg I. Siidra<sup>1,2\*</sup> , Diana O. Nekrasova<sup>1</sup>, Vladimir V. Shilovskikh<sup>3</sup>, Artem S. Borisov<sup>1</sup> and Evgeniya Y. Avdontseva<sup>1</sup>

<sup>1</sup>Department of Crystallography, St. Petersburg State University, University Embankment 7/9, 199034 St. Petersburg, Russia; <sup>2</sup>Kola Science Center, Russian Academy of Sciences, Apatity, Murmansk Region, 184200, Russia; and <sup>3</sup>Geomodel Centre, St. Petersburg State University, University Embankment 7/9, 199034 St. Petersburg, Russia

### Abstract

A new mineral glikinite, ideally  $Zn_3O(SO_4)_2$ , was found in high-temperature exhalative mineral assemblages in the Arsenatnaya fumarole, Second scoria cone of the Great Tolbachik Fissure Eruption (1975–1976), Tolbachik volcano, Kamchatka Peninsula, Russia. Glikinite is associated closely with langbeinite, lammerite- $\beta$ , bradaczekite, euchlorine, anhydrite, chalcocyanite and tenorite. It is monoclinic,  $P2_1/m$ ,  $a = 7.298(18)$ ,  $b = 6.588(11)$ ,  $c = 7.840(12)$  Å,  $\beta = 117.15(3)^\circ$ ,  $V = 335.4(11)$  Å<sup>3</sup> and  $R_1 = 0.046$ . The eight strongest lines of the powder X-ray diffraction pattern [ $d$  in Å ( $I$ ) ( $hkl$ )] are: 6.969(56)(00 $\bar{1}$ ), 3.942(52)(101), 3.483(100)(00 $\bar{2}$ ), 3.294(49)(020), 2.936(43)(120), 2.534(63)(201), 2.501(63)(20 $\bar{3}$ ) and 2.395(86)(02 $\bar{2}$ ). The chemical composition determined by electron-microprobe analysis is (wt.%): ZnO 42.47, CuO 19.50, SO<sub>3</sub> 39.96, total 101.93. The empirical formula calculated on the basis of O = 9 apfu is  $Zn_{2.07}Cu_{0.97}S_{1.98}O_9$  and the simplified formula is  $Zn_3O(SO_4)_2$ . Glikinite is a Zn,Cu analogue of synthetic  $Zn_3O(SO_4)_2$ . The crystal structure of glikinite is based on  $OZn_4$  tetrahedra sharing common corners, thus forming  $[Zn_3O]^{4+}$  chains. Sulfate groups interconnect  $[Zn_3O]^{4+}$  chains into a 3D framework.

**Keywords:** glikinite, new minerals, zinc, sulfates, framework structures, Tolbachik volcano

(Received 8 February 2020; accepted 26 April 2020; Accepted Manuscript published online: 30 April 2020; Associate Editor: Ian T. Graham)

### Introduction

Zinc, along with copper, is one of the predominant metals in arc volcanic emissions (Edmonds *et al.*, 2018). Fumarolic mineral assemblages enriched in zinc have been described from many localities in the world, as in Vulcano (Bernauer, 1936) and Santiaguito (Stoiber and Rose, 1974). Additionally, zinc oxide and zinc silicate condensate particles were detected in considerable amounts in the ashes of Mt St. Helens (Thomas *et al.*, 1982).

Anhydrous sulfate minerals with transition metal cations are dominant in the fumaroles of the Great Tolbachik Fissure eruption, occurring in 1975–1976 and the Tolbachik Fissure eruption of 2012–2013 (Vergasova and Filatov, 2012; Siidra *et al.*, 2017; Pekov *et al.*, 2018a; Siidra *et al.*, 2019). A zinc admixture is very common for many exhalative Cu sulfate minerals (Pekov *et al.*, 2018b). Surprisingly, until recently (Siidra *et al.*, 2018a,b; Siidra *et al.*, 2020), no anhydrous sulfate minerals with Zn-dominated sites in the structure were known and the occurrence of zinkosite,  $ZnSO_4$ , is doubtful to date (Wildner and Giester, 1988).

Herein we report on the chemical composition, structure and properties of glikinite (Cyrillic: гликинит),  $Zn_3O(SO_4)_2$ . Glikinite

is named in honour of Prof Arkady Glikin (Аркадий Эдуардович Гликин) (1943–2012). Arkady Glikin was professor at the Department of Crystallography, Saint-Petersburg State University. The scientific interests of Arkady Glikin were devoted to crystal growth and mineral forming processes. A.E. Glikin was an author of numerous publications in scientific journals, and in 2009 he published a book *Polymineral-Metasomatic Crystallogeneses* (Glikin, 2009). Arkady Glikin was one of the co-authors of the development of the method for obtaining the first synthetic analogue of malachite with jewellery properties. Both the mineral and the mineral name were approved by the Commission on New Minerals, Nomenclature and Classification of the International Mineralogical Association (IMA2018-119, Nazarchuk *et al.*, 2019). Type material is deposited at the Mineralogical Museum, St. Petersburg State University, St. Petersburg, Russia (catalogue no. 1/19693).

### Occurrence and association

Glikinite is a fumarolic mineral that is deposited directly from volcanic gas emissions as a sublimate. It was found in September, 2017 in the Arsenatnaya fumarole, Second scoria cone, Northern Breakthrough (North Breach), Great Fissure eruption, Tolbachik volcano, Kamchatka, Russia. The Second Scoria Cone is located ~18 km SSW of the active shield volcano Ploskiy Tolbachik (Fedotov and Markhinin, 1983). Associated minerals are langbeinite, lammerite- $\beta$ , bradaczekite, euchlorine, anhydrite, chalcocyanite and tenorite (Fig. 1). The temperature of gases at the sampling

\*Author for correspondence: Oleg I. Siidra, Email: o.siidra@spbu.ru

Cite this article: Nazarchuk E.V., Siidra O.I., Nekrasova D.O., Shilovskikh V.V., Borisov A.S. and Avdontseva E.Y. (2020) Glikinite,  $Zn_3O(SO_4)_2$ , a new anhydrous zinc oxysulfate mineral structurally based on  $OZn_4$  tetrahedra. *Mineralogical Magazine* 84, 563–567. <https://doi.org/10.1180/mgm.2020.33>

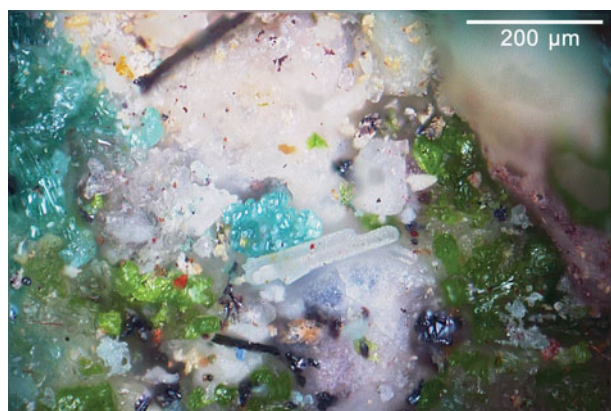


**Fig. 1.** Glikinite (white with bluish tint prismatic crystals in the centre) associating with lammerite- $\beta$  (sky blue), langbeinite (white matrix), euchlorine (grass green) and tenorite (black). Specimen destroyed during analysis, see text.

location was  $\sim 250^\circ\text{C}$ . All the recovered samples were packed and isolated when collected to avoid any contact with the external atmosphere.

### Physical properties

Glikinite crystals are colourless and transparent. The streak is white. The lustre is vitreous. The mineral is non-fluorescent under UV light or an electron beam. Glikinite is brittle. No cleavage and parting were observed, the fracture is uneven. Hardness corresponds to 2–3 on the Mohs' scale. The density could not be measured due to the small sample size. The density calculated from the empirical formula is  $3.98\text{ g cm}^{-3}$ .

Glikinite is optically biaxial (+),  $\alpha = 1.737(2)$ ,  $\beta = 1.686(2)$ ,  $\gamma$  (calc.) =  $1.671(2)$  (589 nm) and  $2V_{\text{calc}} = 54^\circ$ . Dispersion of optical axes is distinct,  $r > v$ . In plane-polarised light, the mineral is non-pleochroic, colourless or with a slight bluish hue.

### Chemical composition

One crystal ( $290\text{ }\mu\text{m} \times 100\text{ }\mu\text{m}$  in size) was mounted in epoxy resin and polished with successively decreasing oil suspensions of diamond powders with the finishing size of  $0.25\text{ }\mu\text{m}$ . The mineral was then analysed by energy-dispersive (EDS) and wavelength-dispersive (WDS) spectrometry. The analyses were obtained using a Hitachi S-3400N scanning electron microscope equipped with an Oxford Instruments X-Max 20 Energy Dispersive Spectrometer (ED,  $n = 8$ ), and Oxford Instruments Inca Wave 500 Wavelength Dispersive Spectrometer (WD,  $n = 4$ ). The ED spectra were obtained under following conditions: 20 kV accelerating voltage, 1.8 nA beam current; defocused beam ( $10\text{ }\mu\text{m}$  spot size); and acquisition time 30 seconds per spectrum. The spectra were processed automatically using the *AzTecEnergy* software package using the *TrueQ* technique. The WD spectra were obtained under following conditions: 20 kV accelerating voltage; 4 nA beam current; 60 seconds per element acquisition time; and matrix correction using the XPP method. Synthetic  $\text{CaSO}_4$  ( $\text{SK}\alpha$ ), Cu metal ( $\text{CuK}\alpha$ ), Zn metal ( $\text{ZnK}\alpha$ ) and Mo metal ( $\text{MoL}\alpha$ ) were used as standards for both EDS and WDS analyses. The mineral is stable under the electron beam; no surface damage was observed after analysis.

**Table 1.** Analytical data (wt.%) ( $n = 12$ ) for glikinite.

Constituent	Mean	Range	S.D.	Probe standard
ZnO	42.47	42.12–43.29	0.345	Metal Zn
CuO	19.50	18.70–20.31	0.182	Metal Cu
$\text{SO}_3$	39.96	38.63–41.28	0.121	Synthetic $\text{CaSO}_4$
Total	101.93			

**Table 2.** Powder X-ray diffraction data for glikinite.

$l_{\text{meas}}$	$l_{\text{calc}}$	$d_{\text{meas}}$	$d_{\text{calc}}$	$h\ k\ l$
<b>56</b>	<b>57</b>	<b>6.9684</b>	<b>6.9760</b>	<b>0 0 <math>\bar{1}</math></b>
14	33	6.4673	6.4941	1 0 0
20	37	4.6255	4.6248	1 1 0
<b>52</b>	<b>53</b>	<b>3.9421</b>	<b>3.9405</b>	<b>1 0 1</b>
38	50	3.9041	3.9037	1 0 $\bar{2}$
20	100	3.6476	3.6488	2 0 $\bar{1}$
<b>100</b>	<b>83</b>	<b>3.4832</b>	<b>3.4880</b>	<b>0 0 2</b>
<b>49</b>	<b>83</b>	<b>3.2943</b>	<b>3.2939</b>	<b>0 2 0</b>
12	40	3.2129	3.2196	2 0 $\bar{2}$
9	6	3.0805	3.0826	0 1 $\bar{2}$
24	36	2.9795	2.9786	0 2 $\bar{1}$
<b>43</b>	<b>49</b>	<b>2.9364</b>	<b>2.9376</b>	<b>1 2 0</b>
27	20	2.6159	2.6154	1 0 2
<b>63</b>	<b>77</b>	<b>2.5335</b>	<b>2.5344</b>	<b>2 0 1</b>
<b>63</b>	<b>71</b>	<b>2.5068</b>	<b>2.5084</b>	<b>2 0 <math>\bar{3}</math></b>
33	98	2.4449	2.4450	2 2 $\bar{1}$
16	18	2.4165	2.4164	1 1 $\bar{3}$
<b>86</b>	<b>77</b>	<b>2.3945</b>	<b>2.3948</b>	<b>0 2 <math>\bar{2}</math></b>
2	3	2.3653	2.3654	2 1 1
2	3	2.3121	2.3124	2 2 0
22	19	2.0800	2.0802	1 3 0
4	6	2.0408	2.0408	3 1 $\bar{3}$
3	1	1.9185	1.9182	1 2 1
15	23	1.8252	1.8244	4 0 $\bar{2}$
10	18	1.8252	1.7983	3 2 $\bar{3}$

The strongest lines are given in bold.

**Table 3.** Crystallographic data and refinement parameters for glikinite.

<b>Crystal data</b>	
Formula	$\text{Zn}_3\text{O}(\text{SO}_4)_2$
Crystal size (mm)	$0.03 \times 0.03 \times 0.15$
Temperature (K)	293
Crystal system, space group	$P2_1/m$
Unit-cell dimensions $a, b, c$ (Å)	7.298(18), 6.588(11), 7.840(12)
$\beta$ (°)	117.15(3)
Unit-cell volume (Å <sup>3</sup> )	335.4(11)
$Z$	2
Calculated density ( $\text{g}\cdot\text{cm}^{-3}$ )	4.00
Absorption coefficient ( $\text{mm}^{-1}$ )	11.29
<b>Data collection</b>	
Radiation, wavelength (Å)	$\text{MoK}\alpha$ , $\lambda = 0.71073$
$\theta$ range (°)	2.920–27.914
$h, k, l$ ranges	$-9 \leq h \leq 9, -6 \leq k \leq 5, -10 \leq l \leq 9$
Total reflections collected	1135
Unique reflections ( $R_{\text{int}}$ )	621 (0.041)
Unique reflections $F > 4\sigma(F)$	518
<b>Structure refinement</b>	
Refinement method	Full-matrix least-squares on $F^2$
Weighting coefficients $a, b$	0.08020, 0.0000
Twin fractions	39:61
Data/restraints/parameters	621/18/80
$R_1$ [ $F > 4\sigma(F)$ ], $wR_2$ [ $F > 4\sigma(F)$ ]	0.046, 0.115
$R_1$ all, $wR_2$ all	0.058, 0.121
Gof on $F^2$	1.02
$\Delta\rho_{\text{max}}, \Delta\rho_{\text{min}}$ ( $\text{e}\ \text{\AA}^{-3}$ )	1.130, -1.450

**Table 4.** Coordinates, isotropic and anisotropic displacement parameters ( $\text{\AA}^2$ ) of atoms in glikinite.

Atom	X	y	z	$U_{eq}$	$U^{11}$	$U^{22}$	$U^{33}$	$U^{23}$	$U^{13}$	$U^{12}$
Zn1	1/2	1/2	0	0.0154(5)	0.0194(13)	0.0102(14)	0.0180(9)	0.0004(9)	0.0097(12)	-0.0022(7)
Zn2	-0.1252(4)	3/4	0.2536(3)	0.0164(7)	0.0181(11)	0.013(2)	0.0123(11)	0	0.0021(9)	0
Zn3	0.6595(4)	3/4	0.7708(3)	0.0172(7)	0.0243(14)	0.015(2)	0.0125(11)	0	0.0089(9)	0
S1	0.3528(6)	3/4	0.3051(7)	0.0114(12)	0.015(2)	0.006(4)	0.011(2)	0	0.0039(17)	0
S2	0.0624(7)	3/4	0.7181(7)	0.0114(12)	0.0151(19)	0.011(4)	0.0064(17)	0	0.0039(17)	0
O1	0.6280(14)	3/4	0.0096(19)	0.009(2)	0.007(4)	0.001(6)	0.013(4)	0	0.001(4)	0
O2	0.1964(14)	0.9312(19)	0.7636(12)	0.017(2)	0.011(4)	0.021(8)	0.013(4)	-0.003(4)	0.000(3)	0.001(4)
O3	-0.079(2)	3/4	0.5212(19)	0.026(4)	0.041(8)	0.010(11)	0.012(6)	0	-0.001(6)	0
O4	0.388(2)	0.570(2)	0.2148(16)	0.032(3)	0.070(9)	0.006(9)	0.042(6)	0.002(5)	0.044(7)	0.004(6)
O5	0.046(2)	3/4	0.8312(19)	0.030(4)	0.023(7)	0.050(12)	0.027(7)	0	0.021(6)	0
O6	0.139(3)	3/4	0.262(3)	0.077(8)	0.042(10)	0.055(17)	0.17(2)	0	0.075(13)	0
O7	0.479(3)	3/4	0.497(2)	0.091(10)	0.14(2)	0.050(19)	0.009(7)	0	-0.032(11)	0

**Table 5.** Selected interatomic distances (in  $\text{\AA}$ ) in glikinite.

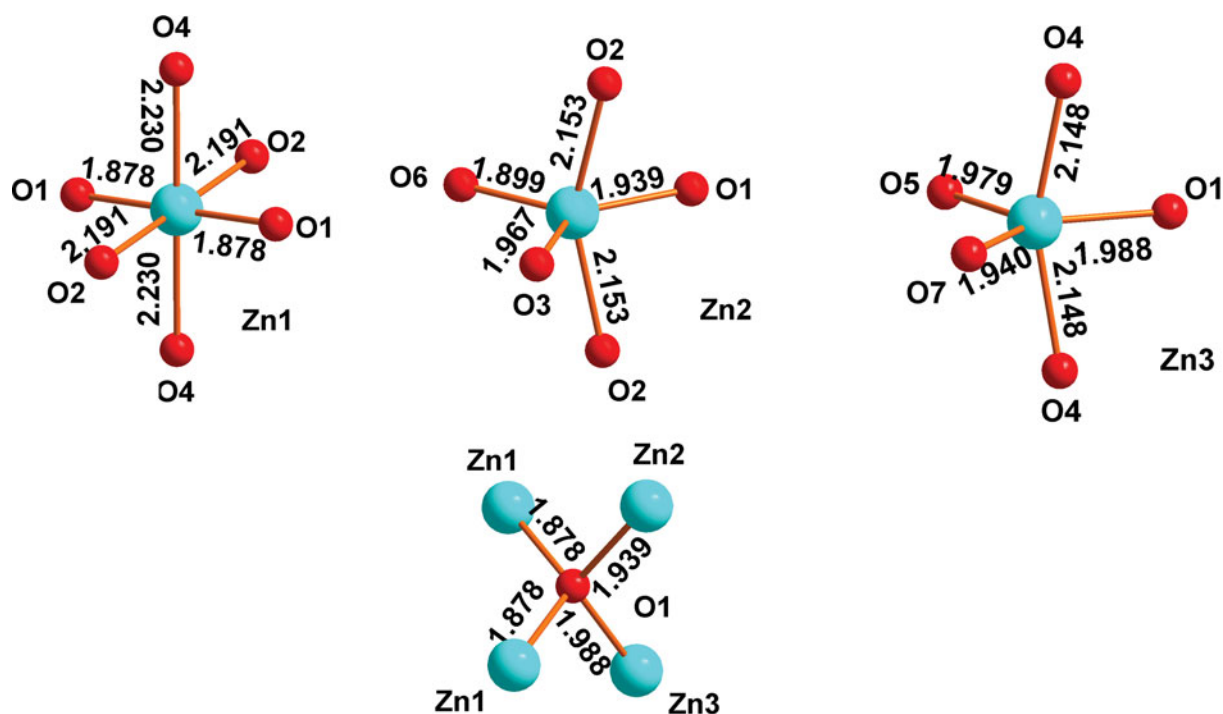
Zn1-O1	1.878(5) × 2	S1-O7	1.361(15)
Zn1-O2	2.191(10) × 2	S1-O6	1.435(18)
Zn1-O4	2.230(10) × 2	S1-O4	1.465(13) × 2
		<S1-O>	1.432
Zn2-O6	1.902(17)	S2-O3	1.413(14)
Zn2-O1	1.939(12)	S2-O5	1.435(13)
Zn2-O3	1.967(14)	S2-O2	1.480(12) × 2
Zn2-O2	2.153(13) × 2	<S2-O>	1.451
Zn3-O7	1.938(15)	O1-Zn1	1.878(5) × 2
Zn3-O5	1.977(14)	O1-Zn2	1.939(12)
Zn3-O1	1.987(13)	O1-Zn3	1.987(13)
Zn3-O4	2.144(15) × 2		

The empirical formula calculated on the basis of O = 9 apfu is  $\text{Zn}_{2.07}\text{Cu}_{0.97}\text{S}_{1.98}\text{O}_9$  (Table 1). The simplified formula is  $(\text{Zn}, \text{Cu})_3\text{O}(\text{SO}_4)_2$  or  $\text{Zn}_3\text{O}(\text{SO}_4)_2$ , which requires  $\text{ZnO} = 60.40$  and  $\text{SO}_3 = 39.60$ , total 100.00 wt.%.

### X-ray crystallography

Powder X-ray studies were carried-out using a Rigaku R-Axis Rapid II diffractometer with a cylindrical image plate detector, using  $\text{CoK}\alpha$  radiation. For the powder-diffraction study, a Gandolfi-like motion on the  $\varphi$  and  $\omega$  axes was used to randomise the sample and observed  $d$  values and intensities were derived using *osc2xrd* software (Britvin *et al.*, 2017). The powder data are presented in Table 2. Unit-cell parameters refined from the powder data are:  $a = 7.287(7) \text{\AA}$ ,  $b = 6.595(8) \text{\AA}$ ,  $c = 7.841(7) \text{\AA}$ ,  $\beta = 117.24(9)^\circ$ ,  $V = 335.0(5) \text{\AA}^3$  and  $Z = 2$ .

The specimen shown in Fig. 1 was destroyed for single-crystal XRD analysis. A prismatic crystal of glikinite was crushed under the microscope into separate thin single-crystal fragments. A thin needle ( $0.03 \times 0.03 \times 0.15 \text{ mm}$ ) was used for diffraction measurements performed on a Bruker Smart Apex II DUO diffractometer with a micro-focus X-ray tube equipped with a CCD detector ( $\text{MoK}\alpha$  radiation). The data were integrated and corrected for absorption using a multi-scan type model implemented in the

**Fig. 2.** Coordination of atoms in glikinite.

**Table 6.** Crystal chemical data for glikinite, the related synthetic compound, and vergasovaite.

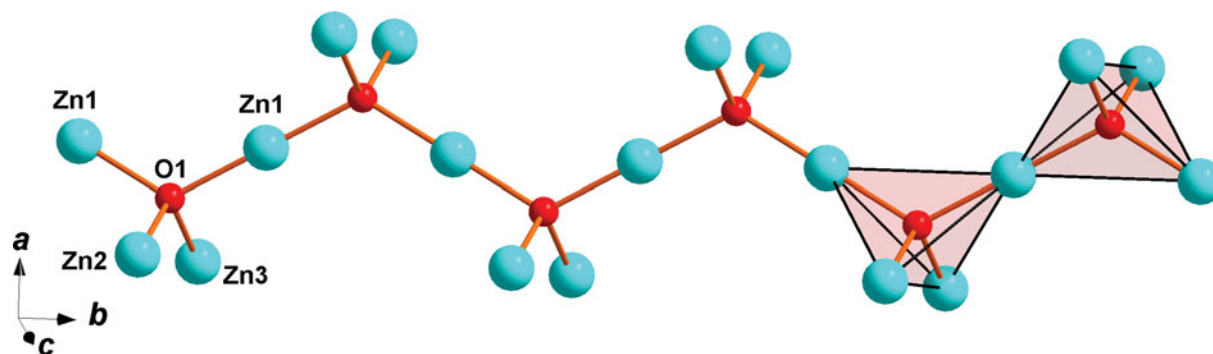
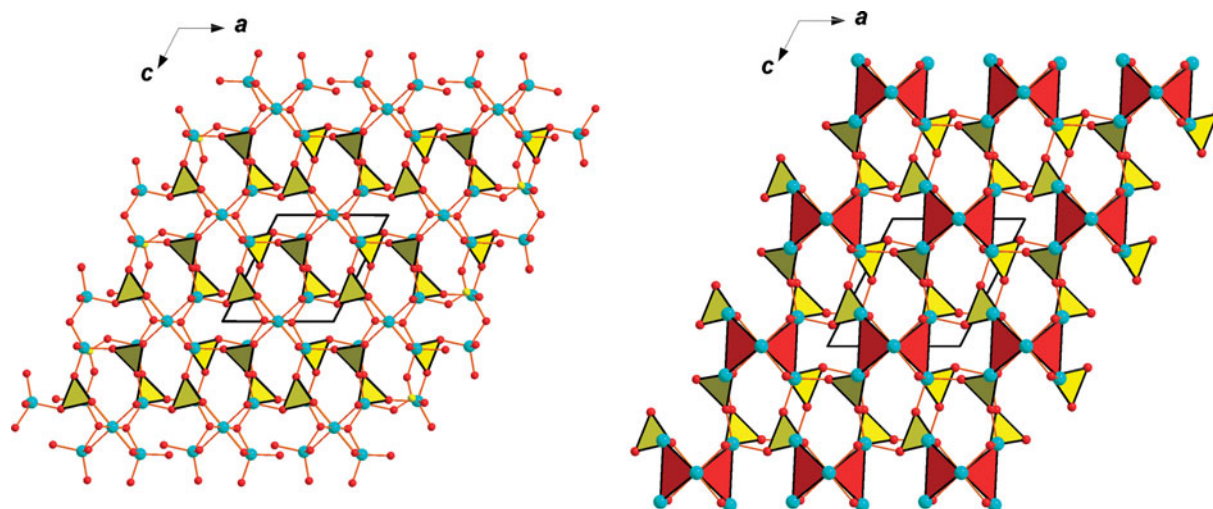
Mineral/ compound	Glikinite	Synthetic	Vergasovaite
Formula	Zn <sub>3</sub> O(SO <sub>4</sub> ) <sub>2</sub>	Zn <sub>3</sub> O(SO <sub>4</sub> ) <sub>2</sub>	Cu <sub>3</sub> O[(Mo,S)O <sub>4</sub> SO <sub>4</sub> ]
Crystal system	Monoclinic	Monoclinic	Orthorhombic
Space group	<i>P2<sub>1</sub>/m</i>	<i>P2<sub>1</sub>/m</i>	<i>Pnma</i>
<i>a</i> , (Å)	7.298(17)	7.937(2)	7.421(2)
<i>b</i> , (Å)	6.588(11)	6.690(2)	6.754(3)
<i>c</i> , (Å)	7.840(12)	7.851(2)	13.624(5)
$\beta$ (°)	117.14(3)	124.39(1)	
<i>V</i> (Å <sup>3</sup> )	335.4(11)	344.01	682.85
<i>Z</i>	2	2	4
<i>R</i> <sub>1</sub>	0.045	0.085	0.067
Reference	This work	Bald and Grün, (1981)	Berlepsch <i>et al.</i> (1999)

Bruker programs *APEX* and *SADABS* (Bruker-AXS, 2014). More than a hemisphere of X-ray diffraction data was collected. The structure was solved by direct methods and was refined using *SHELXL* software (Sheldrick, 2015). All of the atoms were refined anisotropically. The crystal studied was twinned, and the twinning matrix  $[1\ 0\ 0, 0\ \bar{1}\ 0, \bar{1}\ 0\ \bar{1}]$  was employed during the crystal structure refinement. The structure of glikinite was successfully refined using the *SHELX* software package on the basis of  $F^2$  for 518

unique observed reflections with  $F^2 \geq 2\sigma(F^2)$  to  $R_1 = 0.046$  (Table 3). The unit cell of glikinite is similar to that reported for the (apparently isomorphous) synthetic phase Zn<sub>3</sub>O(SO<sub>4</sub>)<sub>2</sub> by Bald and Grün (1981) (*P2<sub>1</sub>/m*,  $a = 7.937(2)$  Å,  $b = 6.690(2)$  Å,  $c = 7.851(2)$  Å,  $\beta = 124.39(1)^\circ$ ,  $V = 344.01$  Å<sup>3</sup> and  $R_1 = 0.085$ ). There is a significant difference in both the *a*-dimension and the monoclinic angle which presumably relates to the significant Cu content in glikinite (Table 1). Atom coordinates and thermal displacement parameters are given in Table 4 and selected interatomic distances in Table 5. The crystallographic information files have been deposited with the Principal Editor of *Mineralogical Magazine* and are available as Supplementary material (see below).

## Discussion

The crystal structure of glikinite contains three symmetrically independent Zn sites with two types of different coordination environments (Fig. 2). The Zn1 site is coordinated by six oxygen ligands thus forming ZnO<sub>6</sub> distorted octahedra. The Zn2 and Zn3 sites have a strongly distorted trigonal bipyramidal coordination environment consisting of five oxygen atoms each. There are two symmetrically independent S sites in the crystal structure of glikinite. The S<sup>6+</sup> cations have typical but distorted tetrahedral coordination. Generally, coordination environments of atoms in

**Fig. 3.** [Zn<sub>3</sub>O]<sup>4+</sup> chain in the structure of glikinite.**Fig. 4.** General projection of the crystal structure of glikinite along the *b* axis. OZn<sub>4</sub> polyhedra are added on the right (SO<sub>4</sub> = yellow and OZn<sub>4</sub> = red).

glikinite are very similar to those in synthetic  $\text{Zn}_3\text{O}(\text{SO}_4)_2$  (Bald and Grünh, 1981). The significant amount of copper determined by microprobe in the structure of glikinite does not significantly influence the bond length and angle values in comparison with the structure of synthetic  $\text{Zn}_3\text{O}(\text{SO}_4)_2$ . The crystal structure of glikinite is an example of a quenched high-temperature structure. Equal distribution of  $\text{Cu}^{2+}$  over three symmetrically independent Zn sites in glikinite can be hypothesised. Thus glikinite is a Zn,Cu analogue of synthetic  $\text{Zn}_3\text{O}(\text{SO}_4)_2$  (Table 6) (Bald and Grünh, 1981).

The structure of glikinite contains seven  $\text{O}^{2-}$  anions. The O2–O7 atoms belong to the sulfate groups. The O1 atoms are tetrahedrally (Fig. 2) coordinated by four Zn atoms forming short and strong O–Zn bonds. From the viewpoint of the bond-valence theory, these bonds are the strongest in the structure and thus it makes sense to consider the  $\text{O}^{2-}$  anions as coordination centres for oxocentred  $\text{O}1\text{Zn}_4$  tetrahedra (Krivovichev *et al.*, 2013).  $\text{OZn}_4$  tetrahedra share common corners thus forming  $[\text{Zn}_3\text{O}]^{4+}$  chains (Fig. 3). A similar topology  $[\text{Cu}_3\text{O}]^{4+}$  of chains was described previously in the structures of vergasovaite  $\text{Cu}_3\text{O}[(\text{Mo},\text{S})\text{O}_4\text{SO}_4]$  (Berlepsch *et al.*, 1999) and kamchatkite  $\text{KCu}_3\text{OCl}(\text{SO}_4)_2$  (Siidra *et al.*, 2017). Sulfate groups interconnect  $[\text{Zn}_3\text{O}]^{4+}$  chains into 3D framework (Fig. 4) in glikinite.

**Supplementary material.** To view supplementary material for this article, please visit <https://doi.org/10.1180/mgm.2020.33>

**Acknowledgements.** We are grateful to an anonymous reviewer, Ian Graham, Stuart Mills and Peter Leverett for valuable comments. This work was financially supported by the Russian Science Foundation, grant no. 16-17-10085. Technical support by the SPbSU X-ray Diffraction and Geomodel Resource Centres is gratefully acknowledged.

## References

- Bald L. and Grünh R. (1981) Die Kristallstruktur von einem Sulfat-reichen Oxidsulfat des Zinks. *Naturwissenschaften*, **68**, 39–39.
- Berlepsch P., Armbruster T., Brugger J., Bykova E.Y. and Kartashov P.M. (1999) The crystal structure of vergasovaite  $\text{Cu}_3\text{O}[(\text{Mo},\text{S})\text{O}_4\text{SO}_4]$ , and its relation to synthetic  $\text{Cu}_3\text{O}(\text{MoO}_4)_2$ . *European Journal of Mineralogy*, **11**, 101–110.
- Bernauer F. (1936) Primäre Teufenunterschiede, Verwitterungs- und Anreicherungs Vorgänge am Krater von Vulcano. *Fortschritte der Mineralogie*, **20**, 31p.
- Britvin S.N., Dolivo-Dobrovolsky D.V. and Krzhizhanovskaya M.G. (2017) Software for processing the X-ray powder diffraction data obtained from the curved image plate detector of Rigaku RAXIS Rapid II diffractometer. *Proceedings of the Russian Mineralogical Society*, **146**, 104–107.
- Bruker-AXS (2014) APEX2. Version 2014.11-0. Madison, Wisconsin, USA.
- Edmonds M., Mather T.A. and Liu E.J. (2018) A distinct metal fingerprint in arc volcanic emissions. *Nature Geoscience*, **11**, 790–794.
- Fedotov S.A. and Markhinin Y.K. (editors) (1983) *The Great Tolbachik Fissure Eruption*. Cambridge University Press, New York.
- Glikin A.E. (2009) Polymineral-metasomatic crystallogenesis. Springer, Dordrecht, 312 p.
- Krivovichev S.V., Mentré O., Siidra O.I., Colmont M. and Filatov S.K. (2013) Anion-centered tetrahedra in inorganic compounds. *Chemical Reviews*, **113**, 6459–6535.
- Nazarchuk E.V., Siidra O.I., Nekrasova D.O., Borisov A.S. and Shilovskikh V.V. (2019) Glikinite, IMA 2018-119. CNMNC Newsletter No. 47, February 2019, page 145; *Mineralogical Magazine*, **83**, 143–147.
- Pekov I.V., Koshlyakova N.N., Zubkova N.V., Lykova I.S., Britvin S.N., Yapaskurt V.O., Agakhanov A.A., Shchিপalkina N.V., Turchkova A.G. and Sidorov E.G. (2018a) Fumarolic arsenates – a special type of arsenic mineralization. *European Journal of Mineralogy*, **30**, 305–322.
- Pekov I.V., Zubkova N.V. and Pushcharovsky D. Yu (2018b) Copper minerals from volcanic exhalations – a unique family of natural compounds: crystal-chemical review. *Acta Crystallographica*, **B74**, 502–518.
- Sheldrick G.M. (2015) Crystal structure refinement with SHELXL. *Acta Crystallographica*, **C71**, 3–8.
- Siidra O.I., Nazarchuk E.V., Zaitsev A.N., Lukina E.A., Avdontseva E.Y., Vergasova L.P., Vlasenko N.S., Filatov S.K., Turner R. and Karpov G.A. (2017) Copper oxosulphates from fumaroles of Tolbachik Vulcano: puninite,  $\text{Na}_2\text{Cu}_3\text{O}(\text{SO}_4)_3$  – a new mineral species and structure refinements of kamchatkite and alumoklyuchevskite. *European Journal of Mineralogy*, **29**, 499–510.
- Siidra O.I., Nazarchuk E.V., Agakhanov A.A., Lukina E.A., Zaitsev A.N., Turner R., Filatov S.K., Pekov I.V., Karpov G.A. and Yapaskurt V.O. (2018a) Hermannjahnite,  $\text{CuZn}(\text{SO}_4)_2$ , a new mineral with chalcocyanite derivative structure from the Naboko scoria cone of the 2012–2013 fissure eruption at Tolbachik volcano, Kamchatka, Russia. *Mineralogy and Petrology*, **112**, 123–134.
- Siidra O.I., Nazarchuk E.V., Lukina E.A., Zaitsev A.N. and Shilovskikh V.V. (2018b) Belousovite,  $\text{KZn}(\text{SO}_4)\text{Cl}$ , a new sulphate mineral from the Tolbachik volcano with apophyllite sheet-topology. *Mineralogical Magazine*, **82**, 1079–1088.
- Siidra O.I., Nazarchuk E.V., Zaitsev A.N. and Shilovskikh V.V. (2020) Majzlanite,  $\text{K}_2\text{Na}(\text{ZnNa})\text{Ca}(\text{SO}_4)_4$ , a new anhydrous sulfate mineral with complex cation substitutions from Tolbachik volcano. *Mineralogical Magazine*, **84**, 153–158.
- Siidra O.I., Borisov A.S., Lukina E.A., Depmeier W., Platonova N.V., Colmont M. and Nekrasova D.O. (2019) Reversible hydration/dehydration and thermal expansion of euchlorine, ideally  $\text{KNaCu}_3\text{O}(\text{SO}_4)_3$ . *Physics and Chemistry of Minerals*, **4**, 403–416.
- Stoiber R.E. and Rose W.I.Jr. (1974) Fumarole incrustations at active Central American volcanoes. *Geochimica et Cosmochimica Acta*, **38**, 495–516.
- Thomas E., Varekamp J.C. and Buseck P.R. (1982) Zinc enrichment in the phreatic ashes of Mt. St. Helens. *Journal of Volcanology and Geothermal Research*, **12**, 339–350.
- Vergasova L.P. and Filatov S.K. (2012) New mineral species in products of fumarole activity of the Great Tolbachik Fissure Eruption. *Journal of Volcanology and Seismology*, **6**, 281–289.
- Wildner M. and Giester G. (1988) Crystal structure refinements of synthetic chalcocyanite ( $\text{CuSO}_4$ ) and zincosite ( $\text{ZnSO}_4$ ). *Mineralogy and Petrology*, **39**, 201–209.